Analysis of STAR-RIS Assisted Downlink CoMP-NOMA Multi-Cell Networks under Nakagami-m Fading

Muhammad Umer ⬤, Muhammad Ahmed Mohsin ⬤, Mikael Gidlund ⬤, *Senior Member, IEEE*
Haejoon Jung ⬤, *Senior Member, IEEE,* and Syed Ali Hassan ⬤, *Senior Member, IEEE*

Abstract—In this letter, we conduct a thorough analytical assessment of a simultaneously transmitting and reflecting reconfigurable intelligent surface (STAR-RIS) assisted non-orthogonal multiple access (NOMA) enhanced coordinated multipoint (CoMP) multi-cell network under Nakagami-m fading. Using the central limit theorem (CLT) and moment-matching based Gamma approximation method, we derive the distributions of effective and cascaded channel gains. Subsequently, leveraging these results, we formulate tractable equations for ergodic rates and outage probabilities across all users in the network. Our analytical results correlate with the simulation results, affirming the efficacy of analytical methodology. Furthermore, the results demonstrate a significant performance improvement of STAR-RIS assisted CoMP-NOMA networks compared to conventional systems.

Index Terms—STAR-RIS, CoMP, NOMA, Nakagami-m fading, ergodic rate, outage probability, Gamma approximation.

I. Introduction

FOR Beyond 5G (B5G) and sixth generation (6G) wireless networks, reconfigurable intelligent surface (RIS) has garnered substantial attention as a prominent solution for enhancing both coverage area and network capacity. Comprised of an array of passive elements, these metasurfaces reflect and transmit incident waves, enhancing the efficiency of wireless signal propagation over an expanded network range. Nonetheless, an inherent limitation of RIS lies in the half-space problem, which results in inadequate signal coverage and degraded performance. Simultaneously transmitting and reflecting (STAR) reconfigurable intelligent surfaces (RIS) can extend the coverage of impinging signals by providing a virtual line-of-sight (vLOS) path to both sides of the metasurface, effectively resolving the half-space problem [1].

Recent studies have shown a growing interest in combining RIS with non-orthogonal multiple access (NOMA). NOMA allows multiple users to operate on shared time-frequeny resources, enhancing spectral efficiency and minimizing network latency [2]. Intending to enhance the performance of multi-cell networks, the integration of coordinated multipoint (CoMP) and NOMA received significant attention [3]. The potential benefits of integrating NOMA, CoMP, and RIS were initially explored in [4]. Another study [5] investigated power allocation and user clustering optimization for CoMP-NOMA networks with RIS, while a group-level successive interference cancellation (SIC) scheme for uplink RIS-assisted CoMP-NOMA networks was proposed in [6].

Most of the previous works suffer from the half-space problem, which limits the coverage area of the RIS and thus rely on optimal placement strategies. The authors in [7] explored the incorporation of STAR-RIS in CoMP-NOMA networks and proposed a joint signal enhancement and interference cancellation scheme. However, the separability of the STAR-RIS elements to serve users belonging to different cells was not considered. Furthermore, an analytical framework to quantify STAR-RIS aided networks is still lacking. To tackle this issue, this letter proposes a tractable analytical framework to evaluate the performance of STAR-RIS assisted CoMP-NOMA networks. First, we use method of moments (MoM) to approximate the effective and cascaded channel gains as Gamma random variables (RVs). Then, tractable expressions for ergodic rate and outage probability are derived for each user. Finally, numerical results are presented to validate the analytical framework and demonstrate the performance gains of STAR-RIS assisted CoMP-NOMA.

II. System Model

As shown in Fig. 1, we consider a multi-cell STAR-RIS assisted CoMP-NOMA network, in which each base station (BS) serves a NOMA pair consisting of its corresponding center and edge users. Consequently, the edge user is part of two NOMA pairs, each served by a different BS. We define the following index sets: $\mathcal{I} = \{1, 2\}$ for the BSs, $C^i = \{1, 2, \ldots, C_i\}$ for the cell-center users of BS_i, and $\mathcal{F} = \{1, 2, \ldots, F\}$ for the cell-edge users. Furthermore, let $\mathcal{U} = {}_{i \in \mathcal{I}} C^i \cup \mathcal{F}$ denote the set of all system users. For ease of exposition, we assume $C_i = 1 \ \forall i \in \mathcal{I}$, and $F = 1$, implying a single cell-center user U_{c_i} per BS_i and a single cell-edge user U_f.

STAR-RIS R comprises K elements and the vector $\mathbf{K}_R^i$ represents the elements assigned to BS_i. In the proposed system model, $\forall i \in \mathcal{I}$, and $\forall u \in \mathcal{U}$, we assume a line-of-sight (LOS) path for links $BS_i - R$, $R - U_u$, and non-line-of-sight (nLOS) path for link $BS_i - U_u$. Furthermore, all LOS links are captured by Nakagami-m fading[1], i.e., $h_{i,R} \sim Nakagami(m_{i,R}, \Omega_{i,R})$, and $h_{R,u} \sim Nakagami(m_{R,u}, \Omega_{R,u})$. Due to the double fading channel, we neglect the impact of the reflected interference

The first two authors contributed equally to this work.

Muhammad Umer, Muhammad Ahmed Mohsin, and Syed Ali Hassan are with the School of Electrical Engineering and Computer Science, National University of Sciences and Technology (NUST), Islamabad 44000, Pakistan (e-mail: {mumer.bee20seecs, mmohsin.bee20seecs, ali.hassan}@seecs.edu.pk).

Mikael Gidlund is with the Department of Computer and Electrial Engineering, Mid Sweden University, 85170 Sundsvall, Sweden (e-mail: mikael.gidlund@miun.se).

Haejoon Jung is with the Department of Electronics and Information Convergence Engineering, Kyung Hee University, Yongin 17104, South Korea (e-mail: haejoonjung@khu.ac.kr).

---

[1]Adopting Nakagami distributions with varying m parameters enables versatile representation of fading channels. For instance, setting $m = 1$ corresponds to modeling Rayleigh fading channels, enhancing the practical applicability of the network.
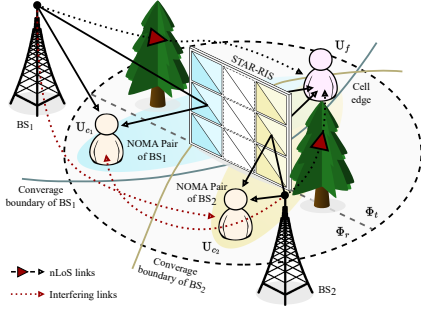
Fig. 1: An illustration of STAR-RIS-aided coordinated NOMA cluster.

link on the performance of cell-center users. The nLOS links are captured by Rayleigh fading, expressed as a special case of Nakagami-m distribution; $h_{i,u} \sim Nakagami(1, \Omega_{i,u})$.

The signal received at U_u, $\forall u \in \mathcal{U}$, can be expressed as

$$y_u = H_{i,u}x_i + H_{i',u}x_{i'} + N_o, \tag{1}$$

where $i' \in \mathcal{I} \setminus \{i\}$, N_o is additive white Gaussian noise (AWGN), i.e., $N_o \sim \mathcal{CN}(0, \sigma^2)$, $x_i = \sqrt{\zeta_{i,c}P_t}x_{i,c} + \sqrt{\zeta_{i,f}P_t}x_f$ is the superimposed signal broadcasted by BS_i, $\zeta_{i,c}$ and $\zeta_{i,f}$ are the power allocation (PA) factors assigned by BS_i to users U_{c_i} and U_f, respectively, and P_t is the total transmit power of each BS. Moreover, $H_{i,u} = h_{i,u} + \mathbf{h_{R,u}^H \Phi_n h_{i,R}}$ denotes the effective channel from BS_i to U_u, where $n = t$ if $u \in C^i$ and $n = r$ if $u \in \mathcal{F}$, representing the transmission and reflection regions of the STAR-RIS. Futhermore, the transmission and reflection coefficient matrices of R are expressed as $\mathbf{\Phi_r} = \sqrt{\beta^r}\text{diag}(e^t j\phi_1^t, e^{j\phi_2^t}, \ldots, e^{j\phi_K^t})$ and $\mathbf{\Phi_t} = \sqrt{\beta^t}\text{diag}(e^{j\phi_1^r}, e^{j\phi_2^r}, \ldots, e^{j\phi_K^r})$, respectively, where β^t, $\beta^r \in [0,1]$ are the amplitude adjustments, satisfying $\beta^t + \beta^r = 1$, and ϕ_k^t, $\phi_k^r \in [0, 2\pi)$, $\forall k \in \mathcal{K} \triangleq \{1, 2, \ldots, K\}$. With the assumption that the perfect CSI is available, the optimal phase shifts can be calculated as $\phi_k^n = \text{mod}[\arg(h_{i,u}) - \arg(h_{i,R} \cdot h_{R,u}), 2\pi]$, which allows us to rewrite the magnitude of the effective channel as $|H_{i,u}| = (|h_{i,u}| + \sqrt{\beta_n}\sum_{k=1}^{K} |h_{R,u}||h_{i,R}|)$.

Following the principle of NOMA, the strong user, U_{c_i}, first decodes U_f's signal and then decodes its own using SIC. The signal-to-interference-plus-noise ratio (SINR) at U_{c_i} for these two processes can be expressed as

$$\gamma_{i,c \to f} = \frac{\zeta_{i,f}\rho|H_{i,c}|^2}{\zeta_{i,c}\rho|H_{i,c}|^2 + \rho|h_{i',c}|^2 + 1}, \tag{2}$$

and

$$\gamma_{i,c} = \zeta_{i,c}\frac{\rho|H_{i,c}|^2}{\rho|h_{i',c}|^2 + 1}, \tag{3}$$

where $\rho = P_t/\sigma^2$ is the transmit SNR of each BS. Unlike U_{c_i}, U_f decodes its own signal directly, and considering non-coherent JT-CoMP, the SINR at U_f can be expressed as [8]

$$\gamma_f = \frac{\zeta_{i,f}\rho|H_{i,f}|^2 + \zeta_{i',f}\rho|H_{i',f}|^2}{\zeta_{i,c}\rho|H_{i,f}|^2 + \zeta_{i',c}\rho|H_{i',f}|^2 + 1}. \tag{4}$$

III. END-TO-END SINR STATISTICS

A. Effective Channel Characterization

Let $Z_{i,u} = |H_{i,u}|^2 = (|h_{i,u}| + \sqrt{\beta_n}\sum_{k=1}^{K} |h_{R,u}||h_{i,R}|)^2$ be the effective channel gain from BS_i to U_u. The following lemma

characterizes the distribution of $Z_{i,u}$.

Lemma 1. *Assuming K, the number of elements in STAR-RIS, is large enough,[2] and by applying MoM, the distribution of $Z_{i,u}$ is approximated as a Gamma distribution, $Z_{i,u} \sim \Gamma\left(k_{Z_{i,u}}, \theta_{Z_{i,u}}\right)$, with the following probability density function (PDF).*

$$f_{Z_{i,u}}(x) = \frac{x^{k_{Z_{i,u}}-1}e^{-\frac{x}{\theta_{Z_{i,u}}}}}{\theta_{Z_{i,u}}^{k_{Z_{i,u}}}\Gamma\left(k_{Z_{i,u}}\right)}, \ x > 0, \tag{5}$$

where $k_{Z_{i,u}} = \frac{\mu_{Z_{i,u}}^2}{\mu_{Z_{i,u}}^{(2)} - \mu_{Z_{i,u}}^2}$ and $\theta_{Z_{i,u}} = \frac{\mu_{Z_{i,u}}^{(2)} - \mu_{Z_{i,u}}^2}{\mu_{Z_{i,u}}}$ are the shape and scale parameters of the Gamma distribution, with
$\mu_{Z_{i,u}} = \frac{2K\sqrt{\beta\Omega_{iu}\Omega_{iR}\Omega_{Ru}}\Gamma_m\left(\frac{1}{2}, \frac{1}{2}, \frac{1}{2}\right)}{\sqrt{m_{iR}m_{Ru}m_{iu}}} + \beta K^2\Omega_{iR}\Omega_{Ru} + \Omega_{iu}$ *and*
$\mu_{Z_{i,u}}^{(2)} = \frac{4\beta^{3/2}K^3\sqrt{\Omega_{iu}}(\Omega_{iR}\Omega_{Ru})^{3/2}\Gamma_m\left(\frac{1}{2}, \frac{3}{2}, \frac{3}{2}\right)}{\sqrt{m_{iu}}(m_{iR}m_{Ru})^{3/2}} + 6\beta K^2\Omega_{iR}\Omega_{iu}\Omega_{Ru} +$
$\frac{4K\Omega_{iu}^{3/2}\sqrt{\beta\Omega_{iR}\Omega_{Ru}}\Gamma_m\left(\frac{3}{2}, \frac{1}{2}, \frac{1}{2}\right)}{\sqrt{m_{iR}m_{Ru}}m_{iu}^{3/2}} + \frac{\beta^2 K^4\Omega_{iR}^2(m_{iR}+1)(m_{Ru}+1)\Omega_{Ru}^2}{m_{iR}m_{Ru}} + \frac{(m_{iu}+1)\Omega_{iu}^2}{m_{iu}}$
as the first and second moment of $Z_{i,u}$, respectively, and $\Gamma_m(a, b, c) = \frac{\Gamma(m_{iu}+a)\Gamma(m_{iR}+b)\Gamma(m_{Ru}+c)}{\Gamma(m_{iu})\Gamma(m_{iR})\Gamma(m_{Ru})}$.

Proof. For brevity, let the combined channel be $G_{i,u} = \sqrt{\beta_n}\sum_{k=1}^{K} |h_{R,u}||h_{i,R}|$. By applying CLT, and noting that it is a scaled double-Nakagami RV, the distribution of $G_{i,u}$ can be approximated as a Gamma distribution, $G_{i,u} \sim \Gamma\left(\frac{\mu_{G_{i,u}}^2}{\mu_{G_{i,u}}^{(2)} - \mu_{G_{i,u}}^2}, \frac{\mu_{G_{i,u}}^{(2)} - \mu_{G_{i,u}}^2}{\mu_{G_{i,u}}}\right)$, where $\mu_{G_{i,u}}$ and $\mu_{G_{i,u}}^{(2)}$ are the first and second moments of $G_{i,u}$, respectively, with the p-th moment of $G_{i,u}$ given by [9] $\mu_{G_{i,u}}^{(p)} = \frac{(K\sqrt{\beta_n})^p(\Omega_{iR}\Omega_{Ru})^{p/2}\Gamma\left(m_{Ru}+\frac{p}{2}\right)\Gamma\left(m_{iR}+\frac{p}{2}\right)}{(m_{Ru}m_{iR})^{p/2}\Gamma(m_{iR})\Gamma(m_{Ru})}$, and as $|h_{i,u}| \sim Nakagami(m_{i,u}, \Omega_{i,u})$, the p-th moments are known to be given by $\mu_{|h_{i,u}|}^{(p)} = \frac{\Gamma\left(m_{iu}+\frac{p}{2}\right)\Omega_{iu}^{p/2}}{\Gamma(m_{iu})m_{iu}^{p/2}}$. Since $|h_{i,u}|$ and $G_{i,u}$ are independent, the p-th moment of $|H_{i,u}|$ can be obtained via the moments of its summands, i.e., $|h_{i,u}|$ and $G_{i,u}$, by applying the binomial theorem. Hence, the p-th moment of $|H_{i,u}|$ is given by

$$\mu_{|H_{i,u}|}^{(p)} = \sum_{q=0}^{p} \binom{p}{q}\mu_{|h_{i,u}|}^{(q)}\mu_{G_{i,u}}^{(p-q)}. \tag{6}$$

Knowing that only the first two moments of $Z_{i,u}$, $\mu_{Z_{i,u}} = \mu_{|H_{i,u}|}^{(2)}$ and $\mu_{Z_{i,u}}^{(2)} = \mu_{|H_{i,u}|}^{(4)}$, are necessary to approximate its distribution as a Gamma distribution, the first two moments of $Z_{i,u}$ are, therefore, given by

$$\mu_{Z_{i,u}} = \mu_{|h_{i,u}|}^{(2)} + 2\mu_{|h_{i,u}|}\mu_{G_{i,u}} + \mu_{G_{i,u}}^{(2)}, \tag{7}$$

$$\mu_{Z_{i,u}}^{(2)} = \mu_{|h_{i,u}|}^{(4)} + 4\mu_{|h_{i,u}|}^{(3)}\mu_{G_{i,u}} + 6\mu_{|h_{i,u}|}^{(2)}\mu_{G_{i,u}}^{(2)}$$
$$+ 4\mu_{|h_{i,u}|}\mu_{G_{i,u}}^{(3)} + \mu_{G_{i,u}}^{(4)}. \tag{8}$$

The final expression of moments can thus be obtained through the means of substitution in (7) and (8). ∎

Note that even in the absence of a direct link, i.e., $|h_{i,u}| = 0$, the effective channel $Z_{i,u}$ is still Gamma distributed, and the rest of the analysis remains valid.

---

[2]CLT and MoM become particularly applicable and yield near accurate results when the number of elements is substantially large ($K >> 1$). This allows for a reliable approximation of the distribution of the variable in question, enhancing the robustness of the statistical analysis.

We proceed to derive the distribution of the sum of a Gamma RV and the square of a Nakagami-m RV each with different shape and scale parameters, further weighted by different constant terms, i.e., path loss and power allocation factors. The details of the derivation are presented in the following lemma.

Lemma 2. *Let* $\mathcal{B}_{i,u}^{(a,b)} = aZ_{i,u} + b|h_{i',u}|^2$, *where* $a, b \in \mathbb{R}^+$, $i' \in \mathcal{I} \setminus \{i\}$, *then the distribution of* $\mathcal{B}_{i,u}^{(a,b)}$ *is approximated as a Gamma distribution,* $\mathcal{B}_{i,u}^{(a,b)} \sim \Gamma\left(k_{\mathcal{B}_{i,u}^{(a,b)}}, \theta_{\mathcal{B}_{i,u}^{(a,b)}}\right)$, *with the following PDF:*

$$f_{\mathcal{B}_{i,u}^{(a,b)}}(x) = \frac{x^{k_{\mathcal{B}_{i,u}^{(a,b)}} - 1} e^{-\frac{x}{\theta_{\mathcal{B}_{i,u}^{(a,b)}}}}}{\theta_{\mathcal{B}_{i,u}^{(a,b)}} \Gamma\left(k_{\mathcal{B}_{i,u}^{(a,b)}}\right)}, \quad x > 0, \quad (9)$$

where $k_{\mathcal{B}_{i,u}^{(a,b)}} = \frac{\mu_{\mathcal{B}_{i,u}^{(a,b)}}^2}{\mu_{\mathcal{B}_{i,u}^{(a,b)}}^{(2)} - \mu_{\mathcal{B}_{i,u}^{(a,b)}}^2}$ *and* $\theta_{\mathcal{B}_{i,u}^{(a,b)}} = \frac{\mu_{\mathcal{B}_{i,u}^{(a,b)}}^{(2)} - \mu_{\mathcal{B}_{i,u}^{(a,b)}}^2}{\mu_{\mathcal{B}_{i,u}^{(a,b)}}}$, *with* $\mu_{\mathcal{B}_{i,u}^{(a,b)}} = a\mu_{Z_{i,u}} + b\Omega_{i,u}$ *and* $\mu_{\mathcal{B}_{i,u}^{(a,b)}}^{(2)} = a^2 \mu_{Z_{i,u}}^{(2)} + 2ab\mu_{Z_{i,u}}\Omega_{i,u} + b^2\Omega_{i,u}^2(1 + \frac{1}{m_{i,u}})$ *as the first and second moments of* $\mathcal{B}_{i,u}^{(a,b)}$, *respectively.*

Proof. As $|h_{i',u}| \sim Nakagami(m_{i',u}, \Omega_{i',u})$, the square of $|h_{i',u}|$ is known to be Gamma distributed, i.e., $|h_{i',u}|^2 \sim \Gamma\left(k_{i',u}, \theta_{i',u}\right)$, where $k_{i',u} = m_{i',u}$ and $\theta_{i',u} = \frac{\Omega_{i',u}}{m_{i',u}}$ are the shape and scale parameters of the Gamma distribution, respectively. Further, by using the scaling property of Gamma distribution, i.e., $X \sim \Gamma(k,\theta) \implies aX \sim \Gamma(k, a\theta)$, the first and second moments of $aZ_{i,u}$ are given by $\mu_{aZ_{i,u}} = a\mu_{Z_{i,u}}$ and $\mu_{aZ_{i,u}}^{(2)} = a^2\mu_{Z_{i,u}}^{(2)}$, respectively. Finally, the first and second moments of $\mathcal{B}_{i,u}^{(a,b)}$ can be obtained by applying the binomial theorem in (6) and substituting the respective moments. ∎

B. Probability Density Functions of SINRs

Lemma 3. *The PDF of the SINR at* U_{c_i} *to decode the signal of* U_f, *i.e.,* $\gamma_{i,c \to f}$, *is given by*

$$f_{\gamma_{i,c \to f}}(x) = \frac{\theta_{\mathcal{W}_{i,c,f}}\left(\frac{x\theta_{\mathcal{W}_{i,c,f}}}{\rho\zeta_{i,f}\theta_{Z_{i,c}}}\right)^{\alpha_{i,c}}\left(\frac{x\theta_{\mathcal{W}_{i,c,f}}}{\rho\zeta_{i,f}\theta_{Z_{i,c}}} + 1\right)^{v_{i,c \to f}}}{\rho\zeta_{i,f}\theta_{Z_{i,c}}B(k_{Z_{i,c}}, k_{\mathcal{W}_{i,c,f}})}, \quad (10)$$

for $x > 0$, *where* $\alpha_{i,c} = k_{Z_{i,c}} - 1$, $v_{i,c \to f} = -(k_{Z_{i,c}} + k_{\mathcal{W}_{i,c,f}})$, $B(\cdot, \cdot)$ *is the Euler Beta function,* $k_{\mathcal{W}_{i,c,f}} = \frac{\mu_{\mathcal{W}_{i,c,f}}^2}{\mu_{\mathcal{W}_{i,c,f}}^{(2)} - \mu_{\mathcal{W}_{i,c,f}}^2}$, *and* $\theta_{\mathcal{W}_{i,c,f}} = \frac{\mu_{\mathcal{W}_{i,c,f}}^{(2)} - \mu_{\mathcal{W}_{i,c,f}}^2}{\mu_{\mathcal{W}_{i,c,f}}}$, *with* $\mu_{\mathcal{W}_{i,c,f}} = \mu_{\mathcal{B}_{i,c}^{(\rho\zeta_{i,c}, \rho)}} + 1$ *and* $\mu_{\mathcal{W}_{i,c,f}}^{(2)} = \mu_{\mathcal{B}_{i,c}^{(\rho\zeta_{i,c}, \rho)}}^{(2)} + 2\mu_{\mathcal{B}_{i,c}^{(\rho\zeta_{i,c}, \rho)}} + 1$.

Proof. The expression in (2) can be rewritten as $\gamma_{i,c \to f} = \frac{\rho\zeta_{i,f}Z_{i,c}}{\mathcal{W}_{i,c,f}}$, where $\mathcal{W}_{i,c,f} = \mathcal{B}_{i,c}^{(\rho\zeta_{i,c}, \rho)} + 1$, with $Z_{i,c}$ and $\mathcal{B}_{i,c}^{(\rho\zeta_{i,c}, \rho)}$ both being Gamma RVs based on the statistics derived in **Lemmas 1** and **2**, respectively. Then, the distribution of $\mathcal{W}_{i,c,f}$ can also be approximated by an equivalent Gamma RV, i.e., $\mathcal{W}_{i,c,f} \sim \Gamma\left(k_{\mathcal{W}_{i,c,f}}, \theta_{\mathcal{W}_{i,c,f}}\right)$. As $Z_{i,c}$ and $\mathcal{W}_{i,c,f}$ are two independent Gamma RVs, the ratio of two Gamma RVs is known to follow a Beta prime distribution, i.e., $\frac{\rho\zeta_{i,f}Z_{i,c}}{\mathcal{W}_{i,c,f}} \sim$

(a) The PDF of $\gamma_{i,c}$ (b) The PDF of $\gamma_{i,c \to f}$ (c) The PDF of γ_f

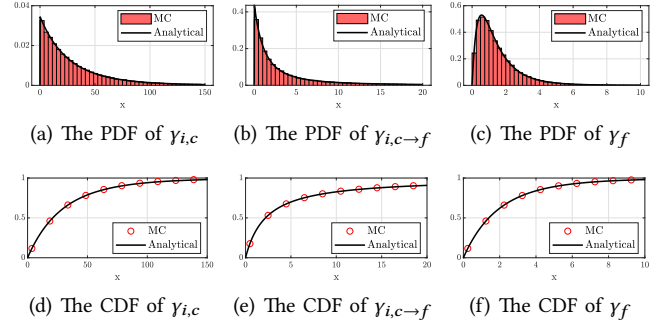(d) The CDF of $\gamma_{i,c}$ (e) The CDF of $\gamma_{i,c \to f}$ (f) The CDF of γ_f

Fig. 2: The PDFs and CDFs of the SINRs at the center and edge user, with $K = 34$ elements, $m_{i,u} = m_{i',u} = 1$, and $m_{i,R} = m_{R,u} = 2$, $\forall i \in \mathcal{I}, i' \in \mathcal{I} \setminus \{i\}$, $\forall u \in \mathcal{U}$.

$\beta'\left(k_{Z_{i,c}}, k_{\mathcal{W}_{i,c,f}}, 1, \rho\zeta_{i,f}\theta_{Z_{i,c}}/\theta_{\mathcal{W}_{i,c,f}}\right)$, corresponding to the PDF in (11). ∎

Corollary 1. *As* $\gamma_{i,c \to f}$ *and* $\gamma_{i,c}$ *are closely related, differing only by weighting constants, the PDF of* $\gamma_{i,c}$ *is given by*

$$f_{\gamma_{i,c}}(x) = \frac{\theta_{\mathcal{W}_{i,c}}\left(\frac{x\theta_{\mathcal{W}_{i,c}}}{\rho\zeta_{i,c}\theta_{Z_{i,c}}}\right)^{\alpha_{i,c}}\left(\frac{x\theta_{\mathcal{W}_{i,c}}}{\rho\zeta_{i,c}\theta_{Z_{i,c}}} + 1\right)^{v_{i,c}}}{\rho\zeta_{i,c}\theta_{Z_{i,c}}B(k_{Z_{i,c}}, k_{\mathcal{W}_{i,c}})}, \quad x > 0, \quad (11)$$

where $v_{i,c} = -(k_{Z_{i,c}} + k_{\mathcal{W}_{i,c}})$, $k_{\mathcal{W}_{i,c}} = \frac{\mu_{\mathcal{W}_{i,c}}^2}{\mu_{\mathcal{W}_{i,c}}^{(2)} - \mu_{\mathcal{W}_{i,c}}^2}$, *and* $\theta_{\mathcal{W}_{i,c}} = \frac{\mu_{\mathcal{W}_{i,c}}^{(2)} - \mu_{\mathcal{W}_{i,c}}^2}{\mu_{\mathcal{W}_{i,c}}}$, *with* $\mu_{\mathcal{W}_{i,c}} = \mu_{\mathcal{B}_{i,c}^{(0, \rho)}} + 1$ *and* $\mu_{\mathcal{W}_{i,c}}^{(2)} = \mu_{\mathcal{B}_{i,c}^{(0, \rho)}}^{(2)} + 2\mu_{\mathcal{B}_{i,c}^{(0, \rho)}} + 1$ *as the first and second moment of* $\mathcal{W}_{i,c} = \mathcal{B}_{i,c}^{(0, \rho)} + 1$, *respectively.*

Lemma 4. *The PDF of the SINR at* U_f, *i.e.,* γ_f, *is given by*

$$f_{\gamma_f}(x) = \frac{\theta_{\mathcal{W}_f}\left(\frac{x\theta_{\mathcal{W}_f}}{\theta_{\mathcal{V}_f}}\right)^{\alpha_f}\left(\frac{x\theta_{\mathcal{W}_f}}{\theta_{\mathcal{V}_f}} + 1\right)^{v_f}}{\theta_{\mathcal{V}_f}B(k_{\mathcal{V}_f}, k_{\mathcal{W}_f})}, \quad x > 0 \quad (12)$$

where $B(\cdot, \cdot)$ *is the Euler Beta function,* $v_f = -(k_{\mathcal{V}_f} + k_{\mathcal{W}_f})$, $k_{\mathcal{V}_f} = \frac{\mu_{\mathcal{V}_f}^2}{\mu_{\mathcal{V}_f}^{(2)} - \mu_{\mathcal{V}_f}^2}$, $\theta_{\mathcal{V}_f} = \frac{\mu_{\mathcal{V}_f}^{(2)} - \mu_{\mathcal{V}_f}^2}{\mu_{\mathcal{V}_f}}$, $k_{\mathcal{W}_f} = \frac{\mu_{\mathcal{W}_f}^2}{\mu_{\mathcal{W}_f}^{(2)} - \mu_{\mathcal{W}_f}^2}$, *and* $\theta_{\mathcal{W}_f} = \frac{\mu_{\mathcal{W}_f}^{(2)} - \mu_{\mathcal{W}_f}^2}{\mu_{\mathcal{W}_f}}$, *with* $\mu_{\mathcal{V}_f} = \rho(\zeta_{i,f}\mu_{Z_{i,f}} + \zeta_{i',f}\mu_{Z_{i',f}})$, $\mu_{\mathcal{V}_f}^{(2)} = \rho^2(\zeta_{i,f}^2\mu_{Z_{i,f}}^{(2)} + 2\zeta_{i,f}\zeta_{i',f}\mu_{Z_{i,f}}\mu_{Z_{i',f}} + \zeta_{i',f}^2\mu_{Z_{i',f}}^{(2)})$, $\mu_{\mathcal{W}_f} = \rho(\zeta_{i,c}\mu_{Z_{i,f}} + \zeta_{i',c}\mu_{Z_{i',f}}) + 1$, *and* $\mu_{\mathcal{W}_f}^{(2)} = 2\mu_{Z_{i,f}}(\rho^2\zeta_{i,c}\zeta_{i',c}\mu_{Z_{i',f}} + \rho\zeta_{i',c} + \rho\zeta_{i,c}) + \rho^2\zeta_{i',c}^2\mu_{Z_{i',f}}^2 + \rho^2\zeta_{i,c}^2\mu_{Z_{i,f}}^2 + 1$.

Proof. The expression in (4) can be rewritten as $\gamma_f = \frac{\mathcal{V}_f}{\mathcal{W}_f}$, where $\mathcal{V}_f = \rho\zeta_{i,f}Z_{i,f} + \rho\zeta_{i',f}Z_{i',f}$ and $\mathcal{W}_f = \rho\zeta_{i,c}Z_{i,f} + \rho\zeta_{i',c}Z_{i',f} + 1$, with $Z_{i,f}$ and $Z_{i',f}$ both being Gamma RVs. The rest of the proof is similar to that of **Lemma 3**. ∎

In Fig. 2, we compare the analytical and simulated PDFs and CDFs of SINRs of network users. The close alignment between the analytical approximations and Monte Carlo (MC) simulations affirms the accuracy of the derived expressions. Additionally, we conduct the *Kolmogorov-Smirnov (KS) goodness-of-fit test*, however, the details are omitted due to space constraints.

IV. Performance Analysis

A. Ergodic Rate (ER)

The ER of the edge user is defined as

$$\mathcal{R}_f = \int_0^\infty \log_2(1+x) f_{\gamma_f}(x)dx, \tag{13}$$

where $f_{\gamma_f}(x)$ is the PDF of γ_f in (12). Noting that the PDF of γ_f is a Beta prime distribution, the ER of the edge user is derived in the following theorem.

Theorem 1. *In the proposed system model, the ER of the edge user is given by*

$$\mathcal{R}_f = \frac{1}{\ln(2)\Lambda_f} G_{3,3}^{3,2}\left(\frac{\theta_{\mathcal{W}_f}}{\theta_{\mathcal{V}_f}} \middle| \begin{array}{c} 0, 1 - k_{\mathcal{W}_f}, 1 \\ 0, 0, k_{\mathcal{V}_f} \end{array}\right), \tag{14}$$

where $G_{p,q}^{m,n}\left(z \middle| \begin{array}{c} a_1, \ldots, a_p \\ b_1, \ldots, b_q \end{array}\right)$ *is the Meijer G-function,* $\Lambda_f = B(k_{\mathcal{V}_f}, k_{\mathcal{W}_f})\,\Gamma(\kappa_f)$ *and* $\kappa_f = k_{\mathcal{V}_f} + k_{\mathcal{W}_f}$.

Proof. Substituting the PDF of γ_f in (12) into (13), we obtain

$$\mathcal{R}_f = \frac{\theta_{\mathcal{W}_f}}{\theta_{\mathcal{V}_f} B(k_{\mathcal{V}_f}, k_{\mathcal{W}_f})} \int_0^\infty \log_2(1+x) \left(\frac{x\theta_{\mathcal{W}_f}}{\theta_{\mathcal{V}_f}}\right)^{\alpha_f}$$
$$\times \left(1 + \frac{x\theta_{\mathcal{W}_f}}{\theta_{\mathcal{V}_f}}\right)^{\nu_f} dx. \tag{15}$$

From [10, Eq. (11)] and [10, Eq. (10)], the logarithmic and power functions can be expressed in terms of a Meijer G-function, i.e., $\log_2(1+z) = G_{2,2}^{1,2}\left(z \middle| \begin{array}{c} 1, 1 \\ 1, 0 \end{array}\right) \middle/ \ln(2)$ and $(1+z)^\nu = G_{1,1}^{1,1}\left(z \middle| \begin{array}{c} 1 - \nu \\ 0 \end{array}\right) \middle/ \Gamma(\nu)$, respectively. Furthermore, using the analytical continuation of the Meijer G-function, the integral in (15) can be rewritten as

$$\mathcal{R}_f = \frac{\theta_{\mathcal{W}_f}}{\ln(2)\theta_{\mathcal{V}_f} B(k_{\mathcal{V}_f}, k_{\mathcal{W}_f})\Gamma(\kappa_f)} \int_0^\infty G_{2,2}^{1,2}\left(x \middle| \begin{array}{c} 1, 1 \\ 1, 0 \end{array}\right)$$
$$\times G_{1,1}^{1,1}\left(\frac{x\theta_{\mathcal{W}_f}}{\theta_{\mathcal{V}_f}} \middle| \begin{array}{c} -k_{\mathcal{W}_f} \\ k_{\mathcal{V}_f} - 1 \end{array}\right) dx. \tag{16}$$

Finally, using the integral representation of the Meijer G-function, we obtain (14). ∎

To gain further insight, we express the high-SNR approximation for the ER of the edge user as

$$\mathcal{R}_f^\infty \approx \frac{1}{\ln(2)\Lambda_{\tilde{f}}} G_{3,3}^{3,2}\left(\theta_{\tilde{f}} \middle| \begin{array}{c} 0, 1 - k_{\tilde{\mathcal{V}}_f}, 1 \\ 0, 0, k_{\mathcal{V}_f} \end{array}\right), \tag{17}$$

where $\Lambda_{\tilde{f}} = B(k_{\mathcal{V}_f}, k_{\tilde{\mathcal{V}}_f})\,\Gamma(\kappa_{\tilde{f}})$, $\kappa_{\tilde{f}} = k_{\mathcal{V}_f} + k_{\tilde{\mathcal{V}}_f}$, and $\theta_{\tilde{f}} = \frac{\theta_{\tilde{\mathcal{V}}_f}}{\theta_{\mathcal{V}_f}}$. The approximate parameters, denoted as $k_{\tilde{\mathcal{V}}_f}$ and $\theta_{\tilde{\mathcal{V}}_f}$, can be computed using the first and second moment, that is, $\mu_{\tilde{\mathcal{V}}_f} = \rho(\zeta_{i,c}\mu_{Z_{i,f}} + \zeta_{i',c}\mu_{Z_{i',f}})$ and $\mu_{\tilde{\mathcal{V}}_f}^{(2)} = \rho^2(\zeta_{i,c}^2\mu_{Z_{i,f}}^{(2)} + 2\zeta_{i,c}\zeta_{i',c}\mu_{Z_{i,f}}\mu_{Z_{i',f}} + \zeta_{i',c}^2\mu_{Z_{i',f}}^{(2)})$, respectively.

Likewise, the ER of the center users is defined as

$$\mathcal{R}_{i,c} = \int_0^\infty \log_2(1+x) f_{\gamma_{i,c}}(x)dx, \tag{18}$$

where $f_{\gamma_{i,c}}(x)$ is the PDF of $\gamma_{i,c}$ in (11). The ER of the center users can then be derived as follows.

Theorem 2. *The ER for the center users is given by*

$$\mathcal{R}_{i,c} = \frac{1}{\ln(2)\Lambda_{i,c}} G_{3,3}^{3,2}\left(\frac{\theta_{\mathcal{W}_{i,c}}}{\rho\zeta_{i,c}\theta_{Z_{i,c}}} \middle| \begin{array}{c} 0, 1 - k_{\mathcal{W}_{i,c}}, 1 \\ 0, 0, k_{Z_{i,c}} \end{array}\right), \tag{19}$$

where $\Lambda_{i,c} = B(k_{Z_{i,c}}, k_{\mathcal{W}_{i,c}})\,\Gamma(\kappa_{i,c})$ *and* $\kappa_{i,c} = k_{Z_{i,c}} + k_{\mathcal{W}_{i,c}}$.

Proof. The proof closely follows that of **Theorem 1**. ∎

Similar insights can be derived for the ER of the center users as of the edge user, however, the details are omitted due to space constraints.

B. Outage Probability (OP)

The OP for the edge user is defined as the probability that the instantaneous SINR at the edge user to decode its own message is below a certain threshold, and can be expressed as $\mathcal{P}_f = \Pr(\gamma_f < \gamma_{th_f})$, where $\gamma_{th_f} = 2^{\mathcal{R}_{th_f}} - 1$ is the target SINR with $\mathcal{R}_{th_f}$ being the target rate for edge users. As $\gamma_f \sim \beta'(k_{\mathcal{V}_f}, k_{\mathcal{W}_f}, 1, \theta_{\mathcal{V}_f}/\theta_{\mathcal{W}_f})$, and the CDF of a Beta prime distribution is known to be an incomplete Beta function, the OP for the edge user can be expressed as

$$\mathcal{P}_f = \frac{\Gamma(k_{\mathcal{V}_f} + k_{\mathcal{W}_f})}{\Gamma(k_{\mathcal{V}_f})\Gamma(k_{\mathcal{W}_f})} B_{\psi_f}(k_{\mathcal{V}_f}, k_{\mathcal{W}_f}), \tag{20}$$

where $\psi_f = \frac{\lambda_{th_f}\theta_{\mathcal{W}_f}}{\theta_{\mathcal{V}_f} + \lambda_{th_f}\theta_{\mathcal{W}_f}}$, and $B_z(\cdot, \cdot)$ is the incomplete Beta function. As the threshold (λ_{th_f}) tends towards infinity, the incomplete Beta function in (20) converges to the Euler Beta function, i.e., $B_{\psi_f}(k_{\mathcal{V}_f}, k_{\mathcal{W}_f}) \to B(k_{\mathcal{V}_f}, k_{\mathcal{W}_f})$.

Similarly, with regards to center users, the OP is defined as the probability that the instantaneous SINR for decoding the user's own message or the message of the edge user falls below a certain threshold. Mathematically, it can be expressed as $\mathcal{P}_{i,c} \approx \Pr(\gamma_{i,c \to f} < \gamma_{th_f}) + \Pr(\gamma_{i,c \to f} > \gamma_{th_f}, \gamma_c < \gamma_{th_c})$, where $\gamma_{th_c} = 2^{\mathcal{R}_{th_c}} - 1$ is the target SINR with $\mathcal{R}_{th_c}$ being the target rate for center users, and the approximate symbol is due to the fact that the detection sequence is not of fully independent events. The first term in the sum expression, denoted here onwards as $\mathcal{P}_{i,c}^{(1)}$, takes on the same form as that of OP for the edge user in (20), except for parameters, i.e., $k_{\mathcal{V}_f} \to k_{Z_{i,c}}$, $k_{\mathcal{W}_f} \to k_{\mathcal{W}_{i,c,f}}$, $\theta_{\mathcal{V}_f} \to \rho\zeta_{i,f}\theta_{Z_{i,c}}$, and $\theta_{\mathcal{W}_f} \to \theta_{\mathcal{W}_{i,c,f}}$. Furthermore, let $\mathcal{P}_{i,c}^{(2)} = \Pr(\gamma_{i,c \to f} > \gamma_{th_f}, \gamma_c < \gamma_{th_c})$, then the second term in the sum expression becomes

$$\mathcal{P}_{i,c}^{(2)} = I_{\psi_{i,c \to f}}(k_{\mathcal{W}_{i,c,f}}, k_{Z_{i,c}}) I_{\psi_{i,c}}(k_{Z_{i,c}}, k_{\mathcal{W}_{i,c}}), \tag{21}$$

where $\psi_{i,c \to f} = \frac{\rho\zeta_{i,f}\theta_{Z_{i,c}}}{\rho\zeta_{i,f}\theta_{Z_{i,c}} + \lambda_{th_f}\theta_{\mathcal{W}_{i,c,f}}}$, $\psi_{i,c} = \frac{\lambda_{th_c}\theta_{\mathcal{W}_{i,c}}}{\rho\zeta_{i,c}\theta_{Z_{i,c}} + \lambda_{th_c}\theta_{\mathcal{W}_{i,c}}}$, and $I_z(\cdot, \cdot)$ is the regularized incomplete Beta function. The OP for the center user is then given by $\mathcal{P}_{i,c} \approx \mathcal{P}_{i,c}^{(1)} + \mathcal{P}_{i,c}^{(2)}$. Further improvement in approximation can be made by making use of the fact that outage performance cannot be better than
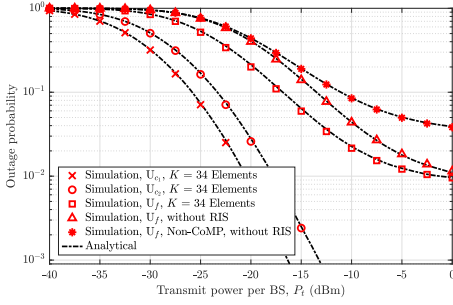
Fig. 3: Outage probability of network users versus P_t for equal amplitude coefficients ($\beta^t = \beta^r$), and element assignments ($\mathbf{K}_R^1 = \mathbf{K}_R^2$), when $K > 0$.

that of the interference-free noise-only case. Therefore, the final expression of the OP can be expressed as the maximum of the two cases, i.e., $\overline{\mathcal{P}_{i,c}} \approx \max\{\mathcal{P}_{i,c}, \Pr\left(\gamma_c < \gamma_{th_c}\right)\}$.

V. Numerical Results

In this section, we present numerical results to validate the accuracy of the derived expressions and gain insight into the performance of the proposed system model. The simulation parameters are as follows: the network operates with a bandwidth of $B = 1$ MHz; AWGN power is configured as $\sigma^2 = -174 + 10\log_{10}(B)$ (dBm) with a noise figure N_f of 12 dB; the power allocation factors for NOMA users, U_{c_i} and U_f, are set to $\zeta_{i,c} = 0.3$ and $\zeta_f = 0.7$, respectively; Nakagami-m fading parameters are set to $m_{i,u} = 1$ and $m_{i,R} = m_{R,u} = 2$ for LOS and nLOS links, respectively.

In Fig. 3, we assess the OP for all users under various transmit power levels (P_t) and system configurations, with fixed thresholds $\lambda_{th_f} = \lambda_{th_c} = 0$ dB. The STAR-RIS assisted CoMP-NOMA network demonstrates significant OP enhancements for U_f, attributed to the formation of vLOS paths. U_{c_1} and U_{c_2} show marginal improvements due to their predominant reliance on direct links from their corresponding BS. Notably, in the absence of CoMP, U_f contends with elevated ICI and consistently high outage probabilities across all power levels.

The impact of the number of RIS elements on the ergodic rate of the network is shown in Fig. 4. We observe that the ergodic rate increases with the number of RIS elements as the RIS elements amplify the channel links. Again, the STAR-RIS assisted CoMP-NOMA network outperforms other networks, due to substantial diversity gains at U_f.

Finally, in Fig. 5, we demonstrate the effect of varying the RIS element assignments ($\mathbf{K}_R^1$, $\mathbf{K}_R^2$) to BS_1 and BS_2, respectively, and the amplitude adjustments (β_t, β_r) in an exhaustive fashion. Notably, the ergodic rate peaks when $\beta_t > \beta_r$ as a result of close proximity of the STAR-RIS to U_f, located within the transmission region of the RIS, thereby defining the optimal configuration for the network. Investigating optimization techniques for STAR-RIS resources can provide further insights to enhance spectral efficiency.

VI. Conclusion

In this letter, we proposed a practical analytical framework designed for STAR-RIS assisted CoMP-NOMA under Nakagami-m fading. By using a moment-matching based
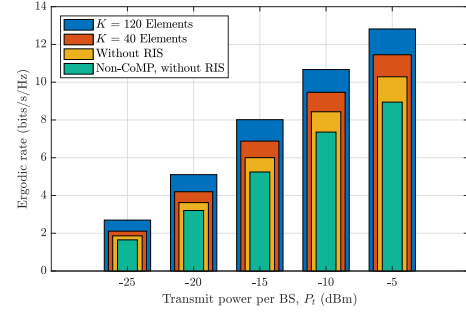

Fig. 4: Ergodic rate comparison of the STAR-RIS assisted CoMP-NOMA system for different system configurations.
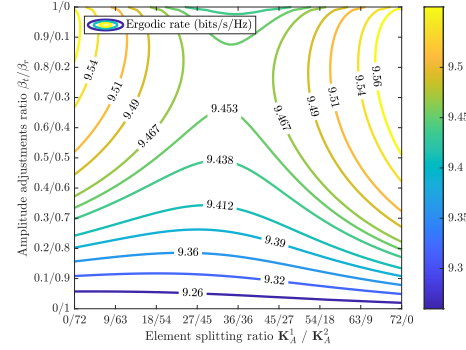

Fig. 5: Ergodic rate for varying RIS element assignments ($\mathbf{K}_R^1$, $\mathbf{K}_R^2$) and amplitude adjustments (β_t, β_r), with $P_t = -10$ dBm.

Gamma approximation, we systematically derived expressions for ergodic rate and outage probability for all the users. To gain deeper insights into network optimization, an exhaustive iterative analysis was performed to maximize data rates.

References

[1] Y. Liu, X. Mu, J. Xu, R. Schober, Y. Hao, H. V. Poor, and L. Hanzo, "STAR: Simultaneous transmission and reflection for 360° coverage by intelligent surfaces," *IEEE Wirel. Commun.*, vol. 28, no. 6, pp. 102–109, 2021.

[2] Z. Ding, Y. Liu, J. Choi, Q. Sun, M. Elkashlan, I. Chih-Lin, and H. V. Poor, "Application of non-orthogonal multiple access in LTE and 5G networks," *IEEE Commun. Mag.*, vol. 55, no. 2, pp. 185–191, 2017.

[3] M. S. Ali, E. Hossain, A. Al-Dweik, and D. I. Kim, "Downlink power allocation for CoMP-NOMA in multi-cell networks," *IEEE Trans. Commun.*, vol. 66, no. 9, pp. 3982–3998, 2018.

[4] M. Elhattab, M.-A. Arfaoui, C. Assi, and A. Ghrayeb, "Reconfigurable intelligent surface assisted coordinated multipoint in downlink NOMA networks," *IEEE Commun. Lett.*, vol. 25, no. 2, pp. 632–636, 2020.

[5] M. Elhattab, M. A. Arfaoui, C. Assi, and A. Ghrayeb, "RIS-assisted joint transmission in a two-cell downlink noma cellular system," *IEEE J. Sel. Areas Commun.*, vol. 40, no. 4, pp. 1270–1286, 2022.

[6] H. Wang, C. Liu, Z. Shi, Y. Fu, and R. Song, "Power minimization for uplink RIS-assisted CoMP-NOMA networks with GSIC," *IEEE Trans. Commun.*, vol. 70, no. 7, pp. 4559–4573, 2022.

[7] T. Hou, J. Wang, Y. Liu, X. Sun, A. Li, and B. Ai, "A joint design for STAR-RIS enhanced NOMA-CoMP networks: A simultaneous-signal-enhancement-and-cancellation-based (SSECB) design," *IEEE Trans. Veh. Technol.*, vol. 71, no. 1, pp. 1043–1048, 2022.

[8] R. Tanbourgi, S. Singh, J. G. Andrews, and F. K. Jondral, "A tractable model for noncoherent joint-transmission base station cooperation," *IEEE Trans. Wirel. Commun.*, vol. 13, no. 9, pp. 4959–4973, 2014.

[9] B. Tahir, S. Schwarz, and M. Rupp, "Analysis of uplink IRS-assisted NOMA under Nakagami-m fading via moments matching," *IEEE Wireless Commun. Lett.*, vol. 10, no. 3, pp. 624–628, 2021.

[10] V. S. Adamchik and O. Marichev, "The algorithm for calculating integrals of hypergeometric type functions and its realization in reduce system," in *Proceedings of the international symposium on Symbolic and algebraic computation*, pp. 212–224, 1990.